Renewal Proposal for IFPRI Project

Modeling porosity development during drying of liquids and slurries

by

Reza Kharaghani

Otto von Guericke University Magdeburg
Chair of Thermal Process Engineering
Drying and Pore Networks Group

November 2025

1. Scientific context and conceptual framework

Foaming spray drying (FSD) is a promising alternative to conventional spray drying with potential energy-efficiency gains. First used in the early 20th century for foamed milk powders with improved flavor and dispersibility [1], it has recently re-emerged for challenging formulations. In FSD, an inert gas (e.g., N_2) is injected into the feed at high pressure (typically > 5 MPa); rapid depressurization at the nozzle then expands the gas and forms fine, foamed particles [2,3]. Comparative works versus conventional spray drying report higher throughput, shorter residence times, and altered particle morphologies [4,5]. Nevertheless, most FSD models remain empirical and product-specific, with limited mechanistic understanding of bubble-drying coupling.

To address this gap, our project has focused on developing a mechanistic understanding and fundamental modeling of drying kinetics and internal morphology evolution in single foaming slurry droplets. This has been a central goal during the initial funding period of this project (September 2023 - October 2026), as such knowledge is essential for the rational design of particles with tailored structures and functionalities produced via foaming spray drying. However, foaming spray drying is governed not only by the behavior of single droplets, but by the dynamics of an entire droplet population. Within this population, numerous coupled physical phenomena take place – inside each droplet, between droplets and the surrounding gas phase, and through droplet-droplet interactions. A comprehensive description of the process therefore requires a multiscale, multiphysics approach.

We have adopted the conceptual framework illustrated in Fig. 1 to address this complexity. The framework links multiple length scales – from the formation of microscopic pores inside single droplets, to the development of pore networks that determine the final particle structure, and ultimately to the collective behavior of many droplets and particles during foaming spray drying. Through this multiscale approach, an integrated picture of how foamed particles and powders are formed can be achieved.

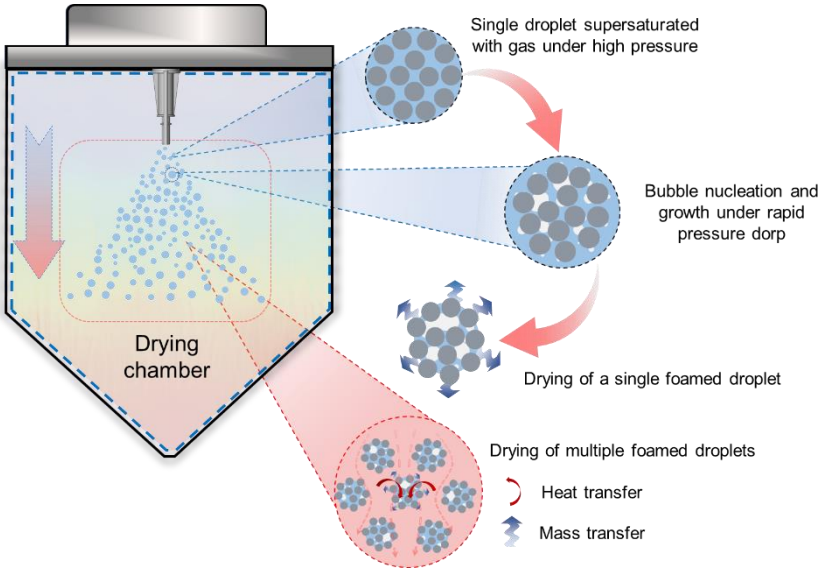

Figure 1: Multiscale approach for predicting drying kinetics and particle morphology during foaming spray drying.

The framework begins with the study of a single droplet, which was the focus of the first funding period. Physical effects occurring within single droplets have been formulated by developing a pore network model (PNM). This model captures the underlying transport and phase-change phenomena in a discrete manner. It operates at the pore scale, where the fluid-filled phase is represented as a network of pores. The solid phase is represented as a complementary network of monosized particles forming a matrix around the pores. Pore sizes are distributed randomly in space, introducing structural disorder. Transport and phase-change processes in both the dispersed and continuous phases are simulated directly (e.g., see [O6, O7], as well as the project reports submitted in 2024 and 2025).

Unique features of this model, as summarized in our 2024 and 2025 reports, include bubble-related events such as bubble nucleation, bubble growth, bubble transport, and bubble coalescence, as well as the coupling of these events with liquid removal and vapor diffusion during drying. During the remaining time of the first funding period (i.e., until October 2026), solid displacement due to capillary forces will be incorporated into the model. With this step, the model will also be able to simulate internal morphology development in single droplets in the presence of bubbles during drying.

While PNM simulations provide essential insights into the pore-scale mechanisms of foaming droplets, their major limitation is the high computational cost. This makes them impractical for direct application at engineering scales. A viable strategy is therefore to perform PNM simulations on representative elementary volumes (REVs), which can be computed within reasonable time, and to use the resulting datasets to estimate effective parameters required in single droplet drying models [O8].

The next step is to transfer the pore-scale information to the droplet scale. This can be done by solving detailed single droplet drying models (SDDMs) – which are typically PDE-based and too complex to be used directly at the spray-dryer scale – by supplying them with the effective parameters derived from PNM simulations. What typically has been done is to reduce SDDMs to characteristic drying curve (CDC) models. After reduction, CDC models can be integrated into tower-scale CFD frameworks**,** followed by experimental validation at the tower scale [O9].

At the tower scale for conventional spray drying, CFD solves macroscopic mass, momentum, and energy balances to estimate airflow, temperature fields, particle size evolution, and humidity-quantities difficult or costly to measure at scale [10]. An Eulerian-Lagrangian framework tracks individual particles and residence times, while particle-level models resolve interphase heat, mass, and momentum exchange plus per-particle force balances. Reviews of gas-flow patterns and tower hydrodynamics are available in [11]. However, CFD accuracy is highly sensitive to feed and particle inputs. Common practice employs empirical correlations (e.g., Ranz–Marshall for heat transfer; Sherwood-based mass transfer) compiled in handbooks and databases [12]. Such approaches treat particles as uniform entities, neglecting internal microstructure that controls true intra-particle transport. Drying kinetics are also

simplified-e.g., via energy-input fits, constant-rate or linear characteristic drying curves (CDC), reaction-engineering approaches, or population-balance models. The most reliable strategy is to incorporate experimentally determined drying kinetics and CDCs from single-droplet studies [O13]. For foam drying, this demands high-resolution datasets capturing its distinct kinetics and CDCs.

2. Core expertise and main results achieved in the first funding phase

The Chair of Thermal Process Engineering (TVT) at Otto-von-Guericke University Magdeburg has longstanding expertise in multiscale heat and mass transfer research, combining experiments, modeling, and simulation for drying, reactions, and particle formation processes such as coating, granulation, and agglomeration in spray dryers and spray fluidized beds (cf. [O14]; www.tvt.ovgu.de). Drying has been a central research topic for decades. Our work spans fundamental studies on mass and heat transport at the pore scale [O15], single-droplet drying investigations [O16], and the complex multi-phase behavior within spray dryers [O17].

At TVT, we developed an in-house CFD model that was first applied to the drying of non-foaming skim milk [O18]. Its development followed a systematic strategy: key drying model parameters were obtained from single-droplet experiments via the characteristic drying curve (CDC) and were subsequently incorporated into the CFD framework. The model has been validated against experiments from our own spray dryer facilities [O13] and and accurately predicts essential process quantities such as air temperatures and moisture content along the tower height, and the mean and variance of the particle size distribution under different operating conditions. Within this framework, obtaining reliable droplet-scale drying parameters – experimentally or through simulation – constitutes the essential first step. This is a core strength of our research group in the context of spray drying.

During the first funding period of the present project, we extended this expertise to foaming slurry droplets and developed a pore network model (PNM) capable of simulating bubble nucleation and growth coupled with drying. The model builds on a pre-existing gas-activation concept (Fig. 2), in which small bubbles remain stabilized in surface cavities under elevated liquid pressure. Upon rapid Upon rapid pressure reduction, the meniscus transitions from concave to convex, and capillary forces may balance the internal gas pressure – thereby triggering bubble activation. The nucleation threshold depends on cavity geometry, surface wettability, and liquid interfacial tension. The PNM identifies such nucleation sites and tracks the dynamic growth of individual bubbles (Fig. 2).

The drying process accompanying bubble formation is also captured by the model. In its current form, the solid matrix is treated as rigid (no capillary-induced deformation). As bubbles expand, liquid is displaced toward the droplet surface. A surface liquid reservoir is therefore included, ensuring saturated surface conditions until it is depleted. Bubble growth changes internal mass transport pathways and is itself

influenced by dissolved-gas availability and transport. Figure 3 illustrates how the predicted liquid distribution differs with and without bubble formation.

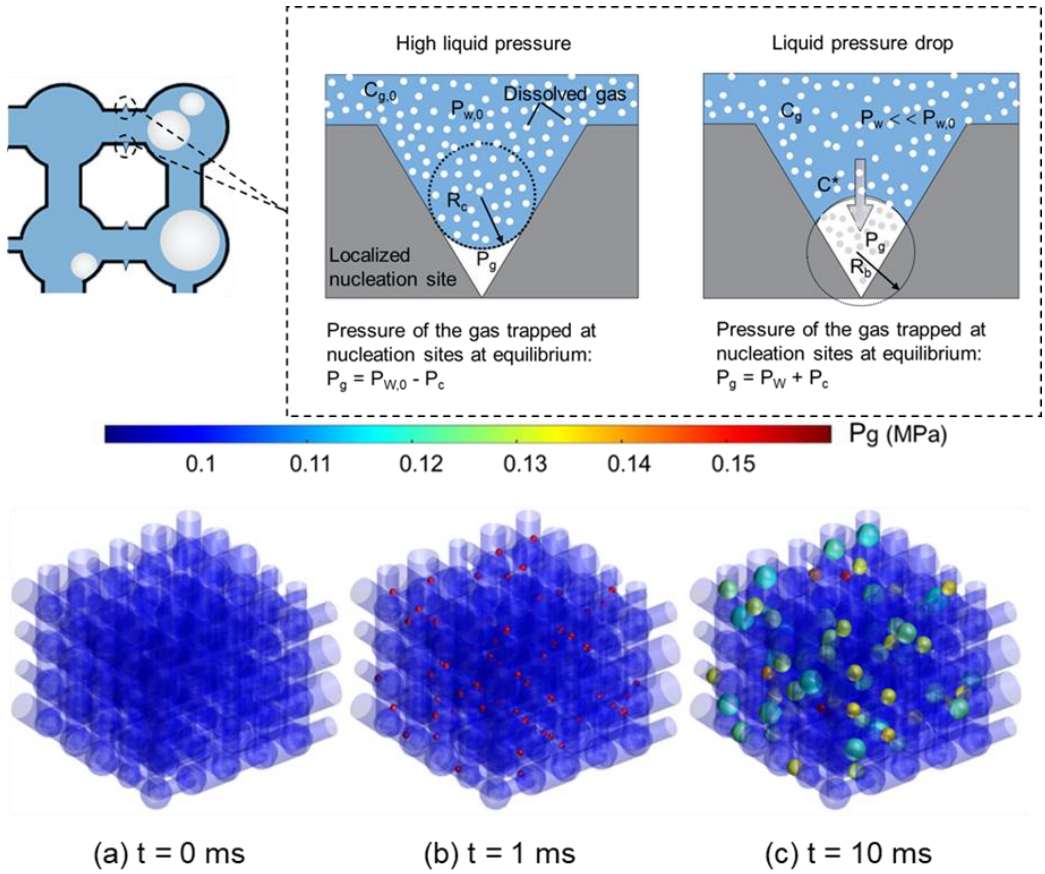

Figure 2: Top row: Schematic of gas trapped within surface cavities under elevated liquid pressure, and the subsequent transition from the meniscus following a rapid pressure drop at a nucleation site. Bottom row: Pore network model simulations of bubble nucleation and growth at successive times: (a) 0 ms (initial), (b) 1 ms (early growth), and (c) 10 ms (advanced growth).

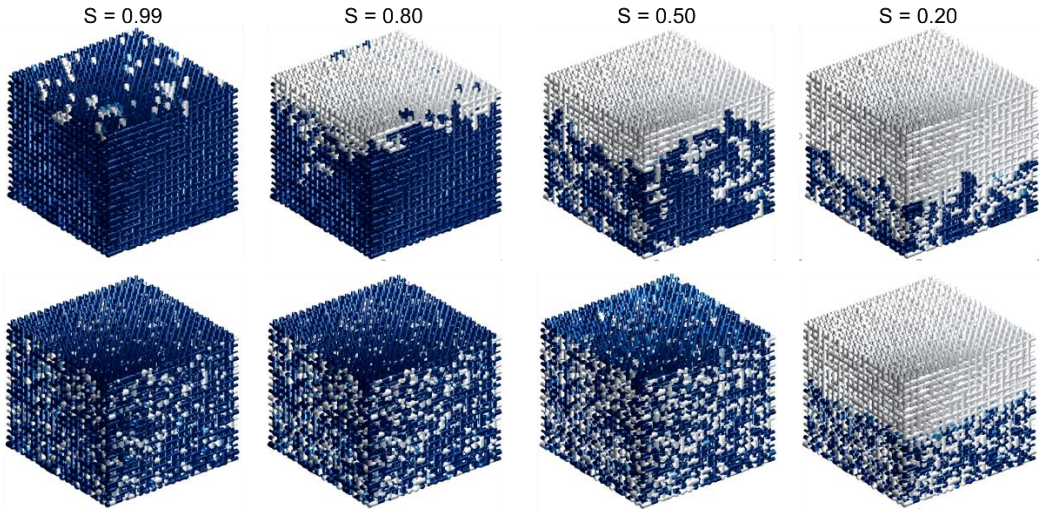

Figure 3: Liquid distribution predicted by the pore network model without bubbles (top) and with bubble formation (bottom). Colored pores indicate liquid-filled regions;

white regions correspond to empty pores and throats. Drying proceeds from the top surface, while all other surfaces are sealed.

In parallel, we extended the regular cubic network to a spatially heterogeneous, random pore network representing a spherical slurry droplet. This structure is generated from the droplet's local solid-concentration field (Fig. 4a) and results in a particle network with a complementary pore network (Fig. 4b). The random PNM has been fully implemented for drying simulations in the presence of bubbles. Figure 4c shows a representative bubble distribution at a network saturation of S = 0.7, where bubbles occupy pores and throats across the network.

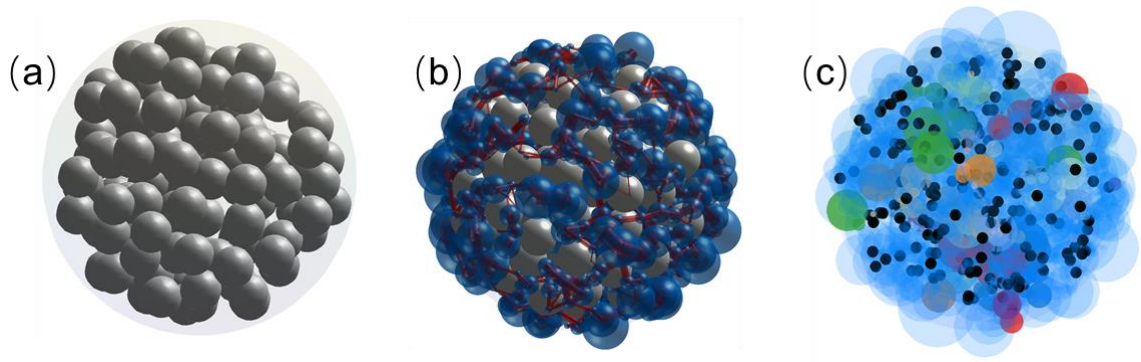

Figure 4: (a) A single slurry droplet containing solid particles, (b) the particle and its complementary pore network, where blue spheres represent pores and red cylinders represent throats, (c) simulated bubble distribution for the network in (b) at a saturation of S = 0.7 during drying. Bubbles forming in pores and throats are shown in green, red, and orange, while black disks indicate solid-particle centers.

In summary, the literature and our preliminary results reveal critical research gaps at multiple scales relevant for foaming spray drying:

- Pore network models with bubbles (pore scale): Our bubble-resolving PNM reproduces drying-induced morphology evolution under given conditions, but quantitative relationships between process parameters and resulting structure are not yet established. These relationships must be mapped into droplet-scale closures to enable multiscale modelling.
- Macroscopic parameters (droplet scale): Morphology-sensitive closures linking operating conditions, drying kinetics, and internal structure evolution are lacking, preventing reliable CFD predictions.
- CFD modelling (tower scale): No validated CFD models currently predict particle moisture and temperature histories, morphology development, or final product properties for foaming spray drying. Missing droplet-scale closures, particularly bubble nucleation, growth, and morphology evolution, are the main limitation.

3. Objectives and work program in the second funding phase

1. Objectives

The aim of this project is to develop high-resolution models capable of predicting drying kinetics and particle morphology evolution during foaming spray drying. The work spans three tightly connected research domains: at the pore scale, pore-network simulations are performed to understand and predict structure evolution driven by bubble nucleation, growth, coalescence, and liquid removal under varying operating conditions (temperature T, liquid surface tension σ, and pressure drop ΔP), yielding effective parameters and closure relationships; at the droplet scale, these macroscopic parameters are used to parameterize both complex and reduced single-droplet drying models that resolve gas-liquid-solid interactions and provide reduced representations such as characteristic drying curves; and at the tower scale, the reduced droplet-level models are incorporated into CFD frameworks to simulate a pilot-scale foaming spray dryer, with predictions of airflow, residence time, moisture evolution, and particle morphology validated against experiments conducted at the same scale.

The central scientific questions to be addressed during the second funding period of this project are as follows:

- How do T, σ, and ΔP govern the morphology (e.g., porosity) of a single slurry droplet with bubbles?
- Which effective parameters/closures are required to upscale from a single slurry droplet to a population of droplets in the dryer within a CFD framework?
- When supplied with the extracted parameters, can the CFD model accurately predict moisture content and particle morphology in agreement with foaming spray drying experiments and product characterizations?

2. Work program including proposed research methods

The work programme begins with WP1 (pore scale), where adaptive pore-network simulations generate high-resolution data on bubble evolution, liquid removal, and structural changes under relevant operating conditions. These simulations provide closure relationships that link material properties and processing parameters to drying kinetics and internal morphology. In WP2 (droplet scale), the resulting datasets are used to extract the effective parameters required for upscaling and to calibrate both detailed and reduced single-droplet drying models. These models then supply the macroscopic descriptions needed in WP3 (tower scale), where they are integrated into an advanced CFD framework to predict moisture histories, residence times, and morphology development during foaming spray drying. Finally, WP4 delivers the experimental measurements required to assess and validate the predictive capability of the tower-scale CFD simulations. The interactions and information flow across the work packages are summarized in Fig. 5.

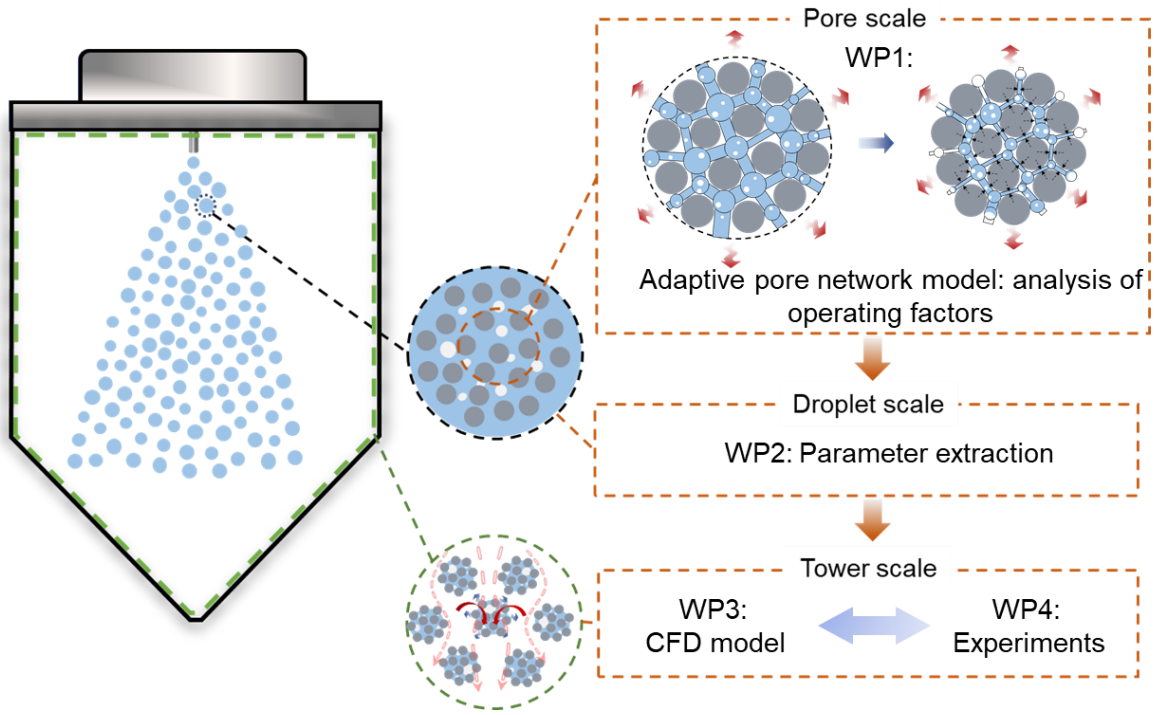

Figure 5: The interactions and information flow among the work packages.

WP1: Generation of data through non-isothermal adaptive pore network model simulations

The adaptive PNM in the first funding period describes the evolution of internal morphology during drying in presence of bubbles. The motion of the solid matrix is driven by capillary forces and the gas pressure inside the bubbles. This motion can cause adjacent pores to expand, shrink, or close. These structural changes, in turn, redistribute the solvent liquid and subsequently modify the drying kinetics. The coupled interactions between bubble dynamics, capillary-driven solid motion, and liquid transport ultimately determine the final particle morphology.

During the first funding period, we identified several key factors influencing bubble formation and drying behavior: liquid surface tension, solids fraction, dissolved gas concentration, and the applied pressure-drop history. With the pore network model, these parameters can be directly linked to drying behavior and to resulting morphological features such as particle size, overall porosity, pore size distribution, and spatial heterogeneity. However, thermal effects were neglected in the first funding period, assuming isothermal conditions. In this work package, the energy balance equations will be incorporated into the existing adaptive pore network model. Heat conduction from neighboring solids and surrounding liquids will be considered when evaluating the temperature profile of solid particles within the droplet. Furthermore, the correlation between saturation vapor pressure and temperature will be included. This addition allows for phase transitions from vapor to liquid when the local vapor pressure exceeds the saturation vapor pressure, which can potentially accelerate the drying process.

During simulations, liquid, bubble, and solid distributions – as well as bubble-gas and dissolved-gas concentrations – will be recorded at fine temporal resolution. Liquid and vapor pressures will also be stored to compute internal liquid and vapor flow rates. Drying rate characteristics (overall drying rate, slope of moisture content vs. time, and surface evaporation rate) will be evaluated separately. The datasets generated in WP1 will form the basis for WP2, where they will be used to compute the effective parameters required for single droplet models, which will subsequently be employed in the CFD simulations of WP3. Two types of solid materials will be simulated in WP1: (i) compressible, soft solids and (ii) stiff, incompressible (rigid) spheres. Considering multiple solid types will allow for a more robust study of the single droplet models in WP2 and the CFD models in WP3.

WP2: Development of complex and reduced models for single foaming droplets

The complex droplet-level models consist of the local saturation (moisture) balance:

$$\frac{\partial}{\partial t}(\varepsilon\rho_w S + \varepsilon\rho_v(1-S)) = -\frac{\partial}{\partial r}(r^2 D(S,T,\varepsilon,)\frac{\partial S}{\partial r}) - \delta, \quad (1)$$

and the energy balance:

$$\frac{dT_p}{\partial t} = \frac{\alpha_p A_p(T_g - T_p) - \dot{M}_v \Delta h_{v,0}}{m_p c_p}, \quad (2)$$

where ρ_w and ρ_v are the liquid solvent and vapor densities, S is the local saturation, and δ represents additional drying contribution arising from bubble expansion. *D* is the effective moisture diffusion coefficient, dependent on local saturation, temperature, porosity, and overall network saturation. T_p and T_g are particle and gas temperatures, respectively. A_p is the droplet surface area, $\Delta h_{v,0}$ is the standard water evaporation enthalpy, α_p is the heat transfer coefficient, and m_p and c_p are the particle and heat capacity. To solve Eqs. (1) and (2) at the droplet level, functional dependencies such as $D(S,T,\varepsilon,)$, $\varepsilon(S)$, $\delta(S)$, $\alpha_p(S)$, and $A_p(S)$ must be determined. These functions are extracted directly from the morphology-resolved PNM data of WP1. Due to the high computational cost of solving Eqs. (1) and (2), these equations should be reduced and then incorporated into a CFD framework.

The mass transfer in the reduced model is expressed as:

$$\dot{M}_v = f A_p \beta_p (C_{v,s} - C_{v,g})\widetilde{M}_v, \quad (3)$$

where $\dot{M}_v$ is the drying rate, β_p is the mass transfer coefficient between the droplet surface and bulk gas, and $C_{v,s}$ and $C_{v,g}$ denote vapor concentration at the surface and in the bulk gas. $\widetilde{M}_v$ is the molecular weight of vapor. The retardation factor f depends on the average moisture content $\overline{X}$ as follows:

$$\bar{X} > \bar{X}_{cr}: f = 1; \quad (4)$$

$$\bar{X} \leq \bar{X}_{cr}: f = f(\bar{X}_{cr}, T, \varepsilon), \quad (5)$$

where $\overline{\mathrm{X}}_{cr}$ is the critical average moisture content, dependent on temperature and porosity. The function f is fitted from the solution of Eqs. (1) and (2). Particle size information in A_p and f is then used in the CFD model.

This approach preserves information on internal morphology evolution – including bubble formation, pore rearrangement, dynamic porosity, and local transport pathways – allowing the CFD model in WP3 to incorporate microstructure-dependent kinetics in a physically consistent manner.

WP3: Advanced tower-scale CFD model

The objective of WP3 is to develop an advanced 3D CFD model for the co-current airflow foaming spray drying process. The model simulates the continuous phase of drying gas (atmospheric air) using an Eulerian approach. The turbulence within the gas phase is modeled with the standard kinetic energy and dissipation rate model. For the dispersed phase, a Lagrangian formulation will describe the motion and drying characteristics. The co-current flow assumption permits neglect of droplet coalescence and particle agglomeration, consistent with the single droplet simulations from WP2. The novelty of WP3 lies in the incorporation of high-resolution drying characteristics of foaming slurry into the CFD model. Data-treatment strategies, such as overall (global) parametric fitting, coarse (regime-wise) fitting, and multi-objective (kinetics + morphology) fitting, will be tested. These inputs come from WP2 (informed by WP1 PNMs). Both particle types from WP1 (compressible vs. rigid) are supported at the spray-dryer scale. Integrating these datasets enables the CFD model to represent particle-scale behaviors that control dryer performance.

The CFD dryer geometry will be constructed based on WP4 to mirror the experimental dryer used in WP4, ensuring that all relevant boundary conditions are defined (e.g., wall-type conditions for the column sides and bottom outlet with zero-velocity boundary constraints, and particle interactions such as bounce-off behavior upon contact with walls). Initial droplet size distributions will be determined based on shadowgraph analysis performed in WP4.

CFD results in WP3 will be validated against experimental data collected in WP4, ensuring predictive accuracy of the model. This high-resolution foaming spray drying model will provide significant potential for optimizing operating parameters to reduce energy input, lower CO_2 emissions, and guide design of particle morphology to meet specific product requirements.

WP4: Experimental validation of tower-scale CFD simulations

The objective of WP4 is to validate the tower-scale CFD predictions developed in WP3 by conducting controlled foaming spray drying experiments. For this purpose, our pilot-scale GEA Niro Mobile Minor™ stainless-steel spray dryer will be retrofitted to handle gas-supersaturated liquids under high pressure (Fig. 6). The retrofit will include the installation of a nitrogen cylinder, a high-pressure gas-liquid mixing device, and a high-pressure feed pump. In addition, the high-pressure atomizer will be

equipped with a 15-µm-diameter diamond nozzle. The GEA Niro high-pressure nozzle option is rated upto 50 MPa. (The installation of extended section)

The Mobile Minor spray dryer has a diameter of 820 mm, a cylindrical section height of 600 mm, and a truncated-cone section height of 690 mm. Further details can be found in [O18]. Two types of liquid-solid systems will be used: (i) reconstituted milk (water + milk solids), and (ii) nanoscale quartz particles with a binder. These two cases serve as validation materials for the WP3 simulations and represent soft (compressible) and hard (incompressible) particle systems, respectively. Liquid systems other than these can be supplied by our industrial partners interested in this project.

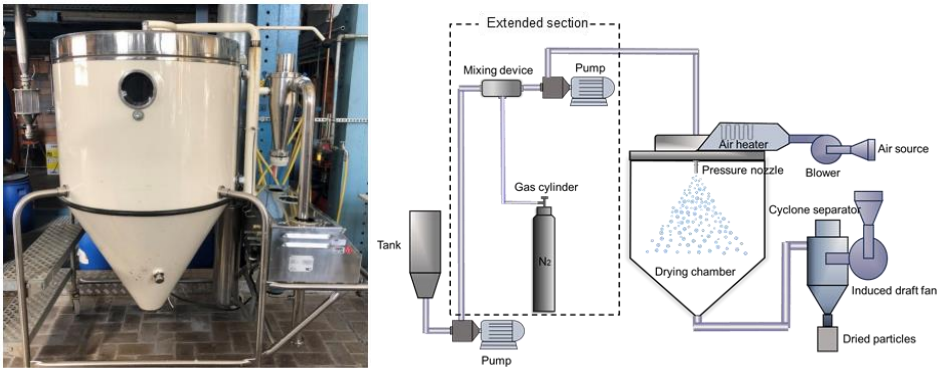

Figure 6: Left: Pilot-scale spray dryer (Mobile Minor, GEA Niro); right: schematic of the extended spray dryer setup to conduct foaming spray drying experiments.

The inlet liquid pressure will be adjustable up to 5 MPa, and diamond-orifice nozzles will ensure reliable atomization under foam-drying conditions used in WP3. Inlet gas temperature, velocity, and humidity will be set to match the boundary conditions used in WP3. By comparing these measurements with the corresponding WP3 predictions, we will assess the predictive accuracy of the CFD model and refine the morphology-informed closures used for foaming spray drying. In parallel, we will request experimental data from the industry partners involved in this project, as these datasets may help evaluate and strengthen the predictive capability of the CFD model developed here.

Table 1: Distribution of work (PNM: pore network model, CFD: computational fluid dynamics) and time schedule for the proposed project.

	1	2	3	4	1	2	3	4	1	2	3	4
WP1: Pore-scale drying data generation												
WP2: Single-droplet model development												
WP3: Tower-scale CFD model development												
WP4: Tower-scale CFD experimental validation												

Project-related publications (O indicates own publications)

[1] Ratti, C., Kudra T.: Drying of foamed biological materials: opportunities and challenges, Drying Technology, 24(2006), 1101-1108.

[2] Zbicinski, I., Rabaeva, J., Lewandowski, A.: Drying of foamed materials, Chapter 6 in Modern Drying Technology, Volume 5: Process Intensification, Wiley-VCH, Weinheim, Germany, 2014

[3] Samborska, K., Poozesh, S., Baranska, A., Sobulska, M., Jedlinska, A., Arpagaus, C., Malekjani, N., Jafari, S.M.: Innovations in spray drying process for food and pharma industries. Journal of Food Engineering, 321(2022), 110960.

[4] Zbicinski, I., Rabaeva J.: Analysis of gas admixing foam spray-drying process. Drying Technology, 28(2009), 103-110.

[5] Lewandowski, A., Maciej, J., Zbiciński, I.: Effect of foam spray drying process parameters on powder morphology. Drying Technology, 37(2019), 535-545.

[O6] Chen, J., Lu, X., Touffet M., Harshe Y., Deleris, I., Kharaghani, A.: Adaptive pore network model for the drying of capillary porous media. Journal of Food Engineering (under review).

[O7] Bałdys, W., Wileńska, M., Bürger, J., Blatkiewicz, M., Piątkowski, M., Sobulska, M., Hashemloo, Z., Kharaghani, A., Jaskulski, M.: Quantitative analysis of key spray drying variables' impact on maltodextrin powder parameters. Drying Technology, 2025 (accepted).

[O8] Bürger, J.V., Jaskulski, M., Kharaghani, A.: Modeling of maltodextrin drying kinetics for use in simulations of spray drying. Drying Technology, 43 (1-2), 214-227.

[O9] Lu, X., Kharaghani, A., Tsotsas, E.: Transport parameters of macroscopic continuum model determined from discrete pore network simulations of drying porous media: Throat-node vs. throat-pore configurations. Chemical Engineering Science, 223(2020), 115723.

[10] Kuriakose, R., Anandharamakrishnan, C.: Computational fluid dynamics (CFD) applications in spray drying of food products. Trends in Food Science & Technology, 21(2010), 383-398.

[11] Don, W.G., Robert, H.P.: Perry's Chemical Engineers' Handbook, Eighth Edition, New York, McGraw-Hill Education, 2008.

[12] Huang, L., Kumar, K., Mujumdar, A.S.: A parametric study of the gas flow patterns and drying performance of co-current spray dryer: Results of a computational fluid dynamics study, Drying Technology, 21(2003), 957-978.

[O13] Tran, T.T.H., Jaskulski, M., Tsotsas, E.: Reduction of a model for single droplet drying and application to CFD of skim milk spray drying, Drying Technology, 35(2017), 1571-1583.

[O14] Bück, A., Tsotsas, E., Sommer, K.: Size enlargement, Ullmann's Encycl. Ind. Chem., 8th ed., Wiley-VCH, 2014.

[O15] Lu, X., Tsotsas, E., Kharaghani, A.: A continuum approach to the drying of small pore networks, Chapter 7 in: Mass Transfer Driven Evaporation from Capillary Porous Media (Eds.: R. Wu, M. Prat), CRC Press, Boca Raton, USA, 2023.

[O16] Peglow, M., Metzger, T., Lee, G., Schiffter, H., Hampel, R., Heinrich, S., Tsotsas, E.: Measurement of average moisture content and drying kinetics for single particles, droplets and dryers, Kapitel 1 in: Modern drying technology, Vol. 2: Experimental Techniques (Eds.: E. Tsotsas, A.S. Mujumdar), 1-71, Wiley-VCH, Weinheim, 2009.

[O17] Jaskulski, M., Kharaghani, A., Tsotsas, E.: Encapsulation methods: Spray drying, spray chilling and spray cooling, Chapter 3 in: Thermal and nonthermal encapsulation methods (Editor: M.K. Krokida), CRC Press, 2017.

[O18] Jaskulski, M., Atuonwu, J.C., Tran, T.T.H., Stapley, A.G.F., Tsotsas, E.: Predictive CFD modeling of whey protein denaturation in skim milk spray drying powder production. Advanced Powder Technology, 28(2017), 3140-3147.